idized. Indeed, most of the basalt samples we studied were taken within just a few kilometers of the axis of the fast-spreading EPR (6), yet all showed NRM unblocking temperatures that extended well beyond the dominant Curie points. The remanence resulting from the single-phase oxidation will be reduced in magnitude by a combination of related mechanisms (14, 15), producing the short-wavelength magnetization contrast required to account for the Central Anomaly magnetic high as the locus of young volcanism. Even if the remanence forms along the ambient external field rather than inheriting the original NRM direction (16), the apparent rapidity of magnetic alteration of the oceanic extrusive source layer as a whole (6, 17) will still result in a high-fidelity recording of the geomagnetic field, as is evident in magnetic anomalies (18).

Although most of the NRM is unblocked by about 300°C in the EPR basalts, some of the remanence typically persists until 525° to 550°C (Fig. 1A, inset). Our experimental results strongly suggest that this remanence is carried by magnetite as a naturally occurring phase (19). Disproportionation of cation-deficient titanomaghemite under sea-floor alteration conditions is a possible and likely explanation for the origin of the magnetite (20), which may result in acquisition of a secondary magnetization [for example, (21)]. An alternative interpretation is that the magnetite represents an original, minor constituent in oceanic basalts (22). The very long-term variations in oceanic basalt magnetization documented in the Deep Sea Drilling Program and Oceanic Drilling Project samples and in amplitudes of marine magnetic anomalies (23) may result from the integrated response of a growing fraction of magnetite to the reversing geomagnetic field, as suggested by the model of Raymond and LaBrecque (24).

REFERENCES AND NOTES

1. M. Talwani, C. C. Windisch, M. G. Langseth Jr., *J. Geophys. Res.* **76**, 473 (1971); T. Atwater and J. D. Mudie, *ibid.* **78**, 8665 (1973).
2. W. O'Reilly, *Rock and Mineral Magnetism* (Chapman & Hall, New York, 1984).
3. E. Irving, *Can. J. Earth Sci.* **7**, 1528 (1970).
4. H. P. Johnson and T. Atwater, *Geol. Soc. Am. Bull.* **88**, 637 (1977).
5. K. C. Macdonald, *ibid.*, p. 541.
6. J. Gee and D. V. Kent, *Geophys. Res. Lett.* **21**, 297 (1994).
7. Detailed rock magnetic experiments were conducted on 10 of the 21 samples described in (6). These include 65 prolonged heating and 15 TRM experiments. Magnetic hysteresis and high-field temperature data were obtained for the entire sample set.
8. M. M. Bina and M. Prévot, *Phys. Earth Planet. Inter.* **54**, 169 (1989).
9. H. C. Soffel and E. Appel, *ibid.* **30**, 348 (1982); B. M. Moskowitz and S. L. Haldegahl, *J. Geophys. Res.* **92**, 10667 (1987).
10. K. J. Gallagher, W. Feitnecht, U. Mannweiler, *Nature* **217**, 1118 (1968).
11. E. C. Stoner and E. P. Wohlfarth, *Philos. Trans. R. Soc. London* **240**, 599 (1948).
12. E. P. Wohlfarth and D. G. Tonge, *Philos. Mag.* **2**, 1333 (1957); I. Joffe and R. Heuberger, *ibid.* **29**, 1051 (1974).
13. J. Gee and D. V. Kent, in preparation.
14. T. Nishitani and M. Kono, *J. Geomagn. Geoelectr.* **41**, 19 (1989).
15. Ö. Özdemir and W. O'Reilly, *Earth Planet. Sci. Lett.* **57**, 437 (1982); J. Housden and W. O'Reilly, *Phys. Earth Planet. Inter.* **64**, 261 (1990).
16. Ö. Özdemir and D. J. Dunlop, *J. Geophys. Res.* **90**, 11513 (1985).
17. J. M. Hall, *J. Geomagn. Geoelectr.* **29**, 411 (1977); H. P. Johnson *et al.*, *Eos* **74**, 620 (1993).
18. S. C. Cande and D. V. Kent, *J. Geophys. Res.* **97**, 15075 (1992).
19. Comparison of zero-field heating and TRM acquisition at 300°C indicates that the generation of new magnetite, as evidenced by large susceptibility increases in the basalt samples, is reflected in the remanent magnetization only if formed or cooled in the presence of an external magnetic field.
20. W. O'Reilly, *Phys. Earth Planet. Inter.* **31**, 65 (1983); J. Housden, A. de Sa, W. O'Reilly, *J. Geomagn. Geoelectr.* **40**, 63 (1988).
21. D. J. Dunlop, *Rep. Prog. Phys.* **53**, 707 (1990).
22. T. Pick and L. Tauxe, *J. Geophys. Res.* **98**, 17949 (1993); *Nature* **366**, 238 (1993).
23. U. Bleil and N. Petersen, *Nature* **301**, 384 (1983); H. P. Johnson and J. E. Pariso, *J. Geophys. Res.* **98**, 435 (1993); T. Furuta, *Geophys. J. Int.* **113**, 95 (1993).
24. C. A. Raymond and J. L. LaBrecque, *J. Geophys. Res.* **92**, 8077 (1987).
25. R. F. Butler and S. K. Banerjee, *ibid.* **80**, 4049 (1975); Ö. Özdemir and W. O'Reilly, *Phys. Earth Planet. Inter.* **25**, 406 (1981).

26. We thank the reviewers for useful comments and C. H. Langmuir and J. F. Bender for the EPR samples. Research was supported by National Science Foundation grant OCE94-02307. This is Lamont-Doherty Earth Observatory contribution 5288.

10 May 1994; accepted 18 July 1994

Rapid Emplacement of Young Oceanic Lithosphere: Argon Geochronology of the Oman Ophiolite

Bradley R. Hacker

$^{40}Ar/^{39}Ar$ dates of emplacement-related metamorphic rocks beneath the Samail ophiolite in Oman show that cooling to <525°C occurred within ~1 million years of igneous crystallization of the ophiolite. This unexpectedly short time span and rapid cooling means that old, cold continental or oceanic lithosphere must have been adjacent to the ophiolite during spreading and then been thrust beneath the ophiolite almost immediately afterward.

Key to understanding how ophiolites—large (up to 50,000 km^2) but thin (<20 km) and dense (3000 to 3300 kg m^{-3}) sheets of oceanic rock—are emplaced onto continental margins (1) is knowing the age of the ophiolite at the time the emplacement process began. Typically, this is achieved by determining when igneous rocks in the ophiolite crystallized at a spreading center and by determining the age of metamorphic rocks associated with the emplacement process. Estimates of such time intervals range from less than 5 million years (My) for the Samail ophiolite, Oman (2, 3), to nearly 20 My for the Bay of Islands, Newfoundland (4), and Brooks Range, Alaska, ophiolites (5). The longer estimates are based on the cooling ages of high-grade metamorphic rocks, which are found beneath most well-preserved ophiolites (6). A short time span means that the ophiolite was young at the time intraoceanic thrusting began and then cooled rapidly. In contrast, a long time span implies that the ophiolite cooled more slowly than normal oceanic lithosphere, retaining heat by some mechanism such as intraoceanic magmatism. It is shown here that the Samail ophiolite was ~1 My old at the time intraoceanic thrusting began.

The Samail ophiolite of Oman and the United Arab Emirates is the best exposed, largest (100 km by 500 km), least deformed, and perhaps most studied ophiolite in the world (7–11). Most of the ophiolite bears the geochemical signature of formation at a mid-ocean-ridge-type spreading center. Younger, volumetrically less substantial volcanic and plutonic rocks may have been derived from subduction zone or within-plate sources (12). Though now distended by normal faulting, the Samail ophiolite is inferred to have been 15 to 20 km thick before its emplacement onto the Arabian craton in Late Cretaceous time (9, 13) (Fig. 1). In all, 7 km of crustal gabbros, sheeted dikes, and volcanic rocks overlie 10 km of tectonized upper mantle peridotite. This entire oceanic lithosphere section was thrust over adjacent oceanic lithosphere and then onto the Arabian craton along a several-hundred-meter-thick shear zone

Geological and Environmental Sciences, Stanford University, Stanford, CA 94305, USA.

composed of partially melted amphibolite-facies mafic rock grading rapidly downward into greenschist facies sedimentary and mafic rocks (*3*, *14*, *15*). The least disrupted section of the metamorphic sole in Oman is exposed above Green Pool along Wadi Tayin. There, tectonized harzburgite overlies 80 m of amphibolite (locally with partial melt leucosomes) that grades down into 145 m of greenschist and, eventually, of relatively unmetamorphosed metasedimentary and metavolcanic rocks (*16*) interpreted as pelagic, slope, rise, and shelf deposits from a Middle Triassic to Late Cretaceous passive margin and ocean basin northeast of the Arabian craton (*7*, *9*, *10*). The amphibolite-facies rocks are believed to represent oceanic gabbro and basalt overridden during the early, intraoceanic thrusting stage of emplacement, whereas the greenschist-facies rocks are inferred to be basalt, clastic sediment, and chert overridden at a later stage before final emplacement on the craton (*3*).

Crystallization ages of the Samail crustal section are well determined by 13 near-concordant U/Pb zircon ages (*17*) from plagiogranites that are interpreted to be late-stage differentiates of gabbros making up most of the plutonic section (*9*, *17*, *18*, *19*). The zircon ages range from 97.3 ± 0.5 to 93.5 ± 0.5 million years ago (Ma) (Fig. 1); 10 of the ages are restricted to a narrow interval of 95.4 ± 0.5 to 94.5 ± 0.5 Ma (2σ standard deviation) and have a mean age of 94.8 Ma. Early stages of the emplacement process are best constrained by K/Ar and $^{40}Ar/^{39}Ar$ ages of minerals from the metamorphic sole. K/Ar ages on hornblende crystals—which are inferred to represent the time of cooling below about 525°C (*20*)—range from 101 to 89 Ma and cluster near 98 Ma (*2*, *9*, *21*, *22*) (Fig. 1). This wide range in hornblende ages implied that formation of the metamorphic rocks was a protracted event (*9*). Moreover, the large uncertainties of these early K/Ar ages (typically with 2σ greater than 6 My) precluded precise measurement of the time interval between igneous crystallization of the ophiolite and subsequent intraoceanic thrusting. Hornblende cooling ages that predate crystallization of the ophiolite crustal sequence posed a particular dilemma, suggesting that the metamorphic rocks might even predate crystallization of the ophiolite (*22*).

I have measured $^{40}Ar/^{39}Ar$ ages on 12 hornblende separates from amphibolites of the metamorphic sole cropping out above Wadi Tayin in the southern part of the ophiolite and near Wadi Sumeini in the north (Table 1) (*23*). The $^{40}Ar/^{39}Ar$ technique can yield precise and potentially more accurate ages than the K/Ar method because the internal concordance of individual gas fractions released from a sample can be evaluated and contributions of excess ^{40}Ar can often be identified. Ten of the 12 hornblende separates yielded plateau or near plateau spectra with weighted mean ages ranging from 95.7 to 92.4 Ma (Fig. 1) (*24*). With 2σ standard deviations as low as 0.6 My, these ages are more precise than most previously measured K/Ar hornblende ages. The ages have a weighted mean of 93.7 Ma, and all except two are externally concordant within 2σ uncertainty (*25*). The remaining two hornblende separates yielded disturbed apparent-age spectra with older ages of ~98 and ~105 Ma. Isotope correlation diagrams (*26*) indicate that at least one of these two samples contains excess ^{40}Ar that contributes to the older apparent ages (*27*). The hornblende samples that lack excess ^{40}Ar are, within error, the same age as or slightly younger than the U/Pb zircon crystallization ages of the ophiolite. All 18 previously published K/Ar ages on Samail metamorphic sole hornblendes (*2*, *9*, *21*, *22*) are concordant with the 10 $^{40}Ar/^{39}Ar$ spectra at the 95% confidence limit—and all except three are concordant at 1σ standard deviation (*28*).

Whereas the U/Pb zircon ages from plagiogranites represent the time of crystallization of Samail oceanic crust (*17*), the cooling ages of hornblendes from the metamorphic sole must slightly postdate

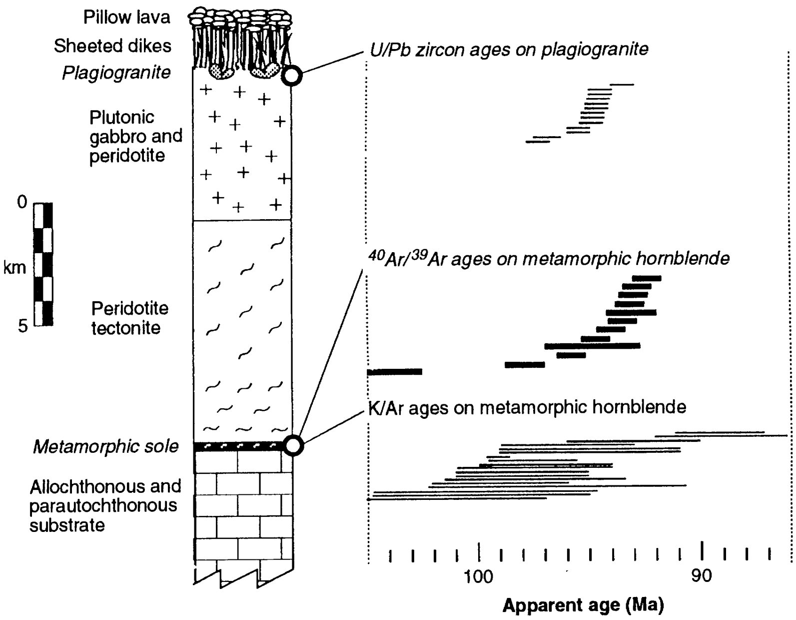

Fig. 1. Comparison of U/Pb zircon ages from plagiogranites (*17*) and $^{40}Ar/^{39}Ar$ ages (discussed here) and K/Ar ages (*2, 9, 21, 22*) from metamorphic sole hornblendes. The line for each age shows 2σ (U/Pb ages) or 1σ (K/Ar and $^{40}Ar/^{39}Ar$ ages) standard deviation of age uncertainty. Other units of the ophiolite substrate are shown in plain text.

Table 1. $^{40}Ar/^{39}Ar$ data. All ages are millions of years. MSWD, mean sum of weighted deviates (goodness of fit) of isochron. Uncertainties are 1σ standard deviations.

Sample	Total fusion age	Weighted mean age	Isochron age	MSWD	$^{40}Ar/^{36}Ar$ intercept
16*	93.7 ± 0.2	93.2 ± 0.3	93.3 ± 0.4	0.9	294 ± 7
19*	90.3 ± 0.5	93.5 ± 0.3	93.6 ± 0.3	0.4	298 ± 3
21*	91.6 ± 0.3	93.0 ± 0.3	92.8 ± 0.3	0.6	301 ± 4
25*	93.1 ± 0.3	94.0 ± 0.3	94.2 ± 0.3	0.7	298 ± 4
32*	94.2 ± 0.6	92.4 ± 0.3	92.6 ± 0.6	3.0	293 ± 3
40†	93.1 ± 0.3	92.8 ± 0.3	92.9 ± 0.3	2.5	279 ± 12
68†	91.7 ± 0.3	95.7 ± 0.3	95.1 ± 0.5	1.3	352 ± 32
142*	92.4 ± 2.1	94.8 ± 1.0	94.6 ± 3.1	0.1	297 ± 16
147*	92.3 ± 1.8	93.2 ± 0.5	92.5 ± 0.6	0.7	351 ± 11
148*	95.1 ± 0.2	94.7 ± 0.3	93.7 ± 1.4	0.1	320 ± 33
		Samples with excess Ar			
56†	104.7 ± 0.4	Not a plateau	54.4	61	1018 ± 511
57†	97.8 ± 0.3	Not a plateau	Poorly defined		

*Wadi Tayin locality; 23°03′N, 58°35′E. †Wadi Sumeini locality, 24°41′N, 56°05′E.

the inception of intraoceanic thrusting. The metamorphic sole formed at an inferred paleodepth of 15 to 20 km (*15*, *29*) and at temperatures (650° to 800°C) (*3*, *9*, *15*, *29*) in excess of those required for Ar diffusion in hornblende (~525°C) (*20*). Near a mature spreading center, temperatures at a depth of 15 km should remain in excess of 1000°C for 2 to 3 My (*30*). Only subduction of colder rock beneath the ophiolite could lower temperatures at a depth of 15 km to 525°C soon after plagiogranites crystallized some 10 km higher in the lithosphere. Assuming closure temperatures of 750°C for Pb diffusion in zircon (*31*) and 525°C for Ar diffusion in hornblende (*20*) and a time difference between mean zircon and hornblende ages (excluding measurement uncertainty) of 1.1 My, the average cooling rate is ~200°C My^{-1}. The elapsed time between the oldest zircon and the youngest hornblende ages is 4.9 My, implying a cooling rate of ~45°C My^{-1}. Expression of these data as cooling rates is somewhat ad hoc because the zircons and hornblendes are separated vertically by 10 km of structural thickness, but at a normal spreading center the temperature was undoubtedly greater at 17 km depth than at the shallower levels of plagiogranite crystallization.

Thus I infer that only 1.1 (+3.9/−1.1) My separated crystallization of oceanic crust and cooling of metamorphic rocks at deep structural levels during intraoceanic thrusting of the Samail ophiolite (*32*). This brief time span requires that (i) the plagiogranite-bearing crustal section and the underlying metamorphic sole are not directly related; (ii) the U/Pb plagiogranite and $^{40}Ar/^{39}Ar$ hornblende ages have been misinterpreted; or (iii) cold material was subducted rapidly beneath an active spreading center. If the plagiogranites and metamorphic sole are unrelated (as in the first case), then their current spatial and temporal relation is fortuitous; this seems unlikely because the metamorphic sole crops out along the length of the ophiolite for 500 km, the dated plagiogranites come from widespread locations in the ophiolite, and the two metamorphic hornblende localities sampled in this study are separated by ~300 km.

Rapid subduction of cold material beneath an active spreading center (as in the third case above) seems incompatible with a typical mid-ocean ridge spreading center. However, the gap of less than a few million years between crystallization of the oceanic crust and cooling at 15 to 20 km depth along the sole thrust can be satisfied only if cold material was thrust beneath the ophiolite concomitant with or immediately after igneous crystallization (*33*). This tight geochronologic constraint does not solve the question of whether the Samail ophiolite formed at a mid-ocean ridge spreading center (*34*) or above a subduction zone (*12*), but it does require that old, cold lithosphere, either continental or oceanic, must have been close to the ophiolite during rifting and then been thrust beneath the huge sheet of dense oceanic lithosphere soon afterward. Another 10 My may have elapsed before final emplacement onto the Arabian craton (*35*).

REFERENCES AND NOTES

1. Ophiolites emplaced on continents are "Tethyan"-type ophiolites, as opposed to "Cordilleran" ophiolites emplaced into accretionary complexes [E. M. Moores, *Rev. Geophys.* **20**, 735 (1982)].
2. M. A. Lanphere, *J. Geophys. Res.* **86**, 2777 (1981); R. Montigny, O. Le Mer, R. Thuizat, H. Whitechurch, *Tectonophysics* **151**, 345 (1988).
3. M. P. Searle and J. Malpas, *Trans. R. Soc. Edinburgh* **71**, 247 (1980).
4. G. R. Dunning and T. E. Krogh, *Can. J. Earth Sci.* **22**, 1659 (1985).
5. K. R. Wirth, J. M. Bird, A. E. Blythe, D. J. Harding, M. T. Heizler, *Tectonics* **12**, 410 (1993).
6. R. A. Jamieson, *J. Metamorph. Geol.* **4**, 3 (1986).
7. K. W. Glennie *et al.*, *Verh. K. Ned. Geol. Mijnbouwkd. Genoot.* **31**, 423 (1974).
8. F. Boudier and A. Nicolas, Eds., *Tectonophysics* **151** (1988).
9. S. J. Lippard, A. W. Shelton, I. G. Gass, *The Ophiolite of Northern Oman* (Geological Society of London Memoir, Blackwell, Oxford, 1986), vol. 11.
10. A. H. F. Robertson, M. P. Searle, A. C. Ries, Eds., *The Geology and Tectonics of the Oman Region* (Geological Society of London, London, 1990), special publication 49.
11. T. Peters, A. Nicolas, R. G. Coleman, *Ophiolite Genesis and Evolution of the Oceanic Lithosphere* (Kluwer, Dordrecht, 1991).
12. Volcanic rocks have been divided into lower, middle, and upper lavas. Although there is agreement that the uppermost, volumetrically least significant lavas erupted from intraplate seamounts, the petrogenesis of the lower and middle lavas is under debate. These rocks have been interpreted as transitional mid-ocean ridge–intraoceanic lavas produced by subduction beneath a spreading center [J. A. Pearce, T. Alabaster, A. W. Shelton, M. P. Searle, *Philos. Trans. R. Soc. London Ser. A* **300**, 299 (1981)] and, alternatively, as the products of mid-ocean ridge spreading and subsequent intraoceanic thrusting [M. Ernewein, C. Pflumio, H. Whitechurch, *Tectonophysics* **151**, 247 (1988); C. Pflumio, in (*11*), vol. 5, pp. 313–351]. Plutonic rocks comprise an early gabbroic series and a late wehrlitic series (*9*, *18*) [P. Browning and J. D. Smewing, *J. Geol. Soc. London* **138**, 279 (1981)]. The early series consists of a gabbro-diorite-plagiogranite suite that was the source of the sheeted dike complex and the lower extrusive unit (*9*) [A. Nicolas and F. Boudier, in (*11*), vol. 5, pp. 39–54]. The wehrlitic series intruded all younger crustal rock types before complete crystallization of the gabbroic sequence and represents 20 to 40% by volume of the plutonic section, is genetically related to most of the upper extrusive sequence, and is inferred to have been emplaced during the initial intraoceanic thrusting stage of ophiolite emplacement (*18*).
13. F. Boudier and R. G. Coleman, *J. Geophys. Res.* **86**, 2573 (1981); N. I. Christensen and J. D. Smewing, *ibid.*, p. 2545; M. H. Manghnani and R. G. Coleman, *ibid.*, p. 2509; J. S. Pallister and C. A. Hopson, *ibid.*, p. 2673.
14. F. Boudier, G. Ceuleneer, A. Nicolas, *Tectonophysics* **151**, 275 (1988).
15. M. Bucher, in (*11*), pp. 543–571.
16. E. D. Ghent and M. Z. Stout, *J. Geophys. Res.* **86**, 2557 (1981).
17. G. R. Tilton, C. A. Hopson, J. E. Wright, *ibid.*, p. 2763.
18. T. Juteau, M. Ernewein, I. Reuber, H. Whitechurch, R. Dahl, *Tectonophysics* **151**, 107 (1988).
19. I. Reuber, *ibid.*, pp. 137–165. At least one of the plagiogranites dated by Tilton *et al.* (*17*) is inferred to be part of the later wehrlitic suite, but the zircon from this body is the same age as that of the plagiogranites inferred to be part of the main gabbroic series.
20. T. M. Harrison, *Contrib. Mineral. Petrol.* **78**, 324 (1981).
21. F. Allemann and T. Peters, *Eclogae Geol. Helv.* **65**, 657 (1972); M. P. Searle, S. J. Lippard, J. D. Smewing, D. C. Rex, *J. Geol. Soc. London* **137**, 589 (1980).
22. E. Gnos and T. Peters, *Contrib. Mineral. Petrol.* **113**, 325 (1993).
23. We irradiated the samples in the TRIGA reactor at Oregon State University using Taylor Creek sanidine as an irradiation flux monitor, which has an assumed age of 27.92 Ma. They were analyzed at Stanford University in a double-vacuum Staudacher-type resistance furnace in cycles with 10 min of heating, 5 to 10 min of gettering with hot TiZrAl, and 6 to 12 min of static analysis in an MAP-216 spectrometer. Further analytical details can be found in B. R. Hacker, *Geol. Soc. Am. Bull.* **105**, 637 (1993).
24. "Plateau" and "near plateau" describe spectra containing three or more contiguous steps that comprise >50% of the total ^{39}Ar released and are internally concordant at the 95% and 67% confidence limits, respectively.
25. The mean isochron and total fusion ages are 93.4 Ma. Mean ages computed only with samples with 2σ uncertainty ≤0.6 My are identical.
26. J. C. Roddick, R. A. Cliff, D. C. Rex, *Earth Planet. Sci. Lett.* **48**, 185 (1980).
27. Argon in a crystal is either trapped at the time of crystallization, produced later by in situ decay of ^{40}K, or diffuses into the crystal from an external source. If the Ar present is a mixture of only two components—one with a radiogenic signature reflecting the age of the sample and identifiable by ^{39}Ar produced during neutron irradiation of K, and the other with a nonradiogenic signature identifiable by the presence of ^{36}Ar—then in principle those two components can be resolved with two-variable correlation tests. Correlation of $^{36}Ar/^{40}Ar$ with $^{39}Ar/^{40}Ar$ revealed a trapped $^{40}Ar/^{36}Ar$ component with a ratio of ~1000 in one of the older samples, considerably greater than the ratio in atmosphere, which is 295.5.
28. Two previously reported K/Ar ages are older than the zircon crystallization ages and likely reflect excess Ar, whereas the one sample that is notably younger may indicate Ar loss.
29. E. Gnos, thesis, University of Bern (1992).
30. B. Parsons and J. G. Sclater, *J. Geophys. Res.* **82**, 803 (1977).
31. E. D. Ghent, M. Z. Stout, R. R. Parrish, in *Short Course on Heat, Metamorphism, and Tectonics*, E. G. Nisbet and C. M. R. Fowler, Eds. (Mineralogical Association of Canada, Saint John's, 1988), pp. 155–188.
32. Assuming mean zircon and hornblende ages of 94.8 and 93.7 Ma, the mean time span was 1.1 My; the maximum time encompassed by the entire range of zircon and hornblende ages is 97.3 − 92.4 My, or 4.9 My; the minimum time is 0 because the oldest hornblende predates the youngest zircon age.
33. B. R. Hacker, *J. Geophys. Res.* **95**, 4895 (1990); *Tectonics* **10**, 455 (1991).
34. F. Boudier *et al.*, *Earth Planet. Sci. Lett.* **75**, 215 (1985).
35. The youngest intraplate lavas that erupted through the ophiolite are reversely magnetized, implying that they are younger than the end of the Cretaceous normal polarity superchron, or <83 Ma [M. Perrin, M. Prevot, F. Bruere, *Tectonophysics* **229**, 31 (1994)].

36. Reviewed by R. G. Coleman, W. G. Ernst, E. D. Ghent, E. Gnos, C. A. Hopson, J. G. Liou, M. O. McWilliams, J. L. Mosenfelder, A. Nicolas, Tj. Peters, and M. P. Searle. Supported by NSF grant EAR 9204741.

22 April 1994; accepted 21 July 1994